HHS Public Access

Author manuscript

Neuroscience. Author manuscript; available in PMC 2017 June 02.

Published in final edited form as:

Neuroscience. 2016 June 2; 324: 399–406. doi:10.1016/j.neuroscience.2016.03.037.

Characterization of cognitive impairments and neurotransmitter changes in a novel transgenic mouse lacking *Slc10a4*

Erica J. Melief[a], **Jeffrey T. Gibbs**[a], **Xianwu Li**[a], **R. Garrett Morgan**[a], **C. Dirk Keene**[a], **Thomas J. Montine**[a], **Richard D. Palmiter**[b,c], and **Martin Darvas**[a]

[a]Department of Pathology, University of Washington, Seattle WA 98104

[b]Department of Biochemistry, University of Washington, Seattle WA 98104

[c]Howard Hughes Medical Institute, University of Washington, Seattle WA 98104

Abstract

An orphan member of the solute carrier family SLC10, SLC10A4 has been found to be enriched in midbrain and brainstem neurons and has been found to co-localize with and to affect dopamine homeostasis. We generated an SLC10A4 knockout mouse (*Slc10a4*$^{\Delta/\Delta}$) using Cre targeted recombination, and characterized behavioral measures of motor and cognitive function as well as dopamine and acetylcholine levels in midbrain and brainstem. In agreement with previous studies, *Slc10a4* mRNA was preferentially expressed in neurons in the brains of wild-type (*Slc10a4*$^{+/+}$) mice and was enriched in dopaminergic and cholinergic regions. *Slc10a4*$^{\Delta/\Delta}$ mice had no impairment in motor function or novelty-induced exploratory behaviors but performed significantly worse in measures of spatial memory and cognitive flexibility. *Slc10a4*$^{\Delta/\Delta}$ mice also did not differ from *Slc10a4*$^{+/+}$ in measures of anxiety. HPLC measures on tissue punches taken from the dorsal and ventral striatum reveal a decrease in dopamine content and a corresponding increase in the metabolite DOPAC, indicating an increase in dopamine turnover. Punches taken from the brainstem revealed a decrease in acetylcholine as compared with *Slc10a4*$^{+/+}$ littermates. Together, these data indicate that loss of SLC10A4 protein results in neurotransmitter imbalance and cognitive impairment.

Keywords

SLC10A4; dopamine; acetylcholine; cognitive impairment; Learning; knockout

Correspondence: Martin Darvas (206-897-5581), mdarvas@uw.edu, Department of Pathology, University of Washington, Seattle 98104.

The authors report no potential conflicts of interest.

INTRODUCTION

During normal cell function, transport of proteins, compounds, and sugars across cell membranes is crucial to maintaining proper signaling. One of the primary mechanisms of transport across cell membranes are proteins that belong to the superfamily of solute carriers (SLCs), which comprises over 300 different proteins and vary greatly in their expression and function (Lin et al., 2015). Members of this family of transporters are the primary conveyance for neurotransmitters across cell membranes, resulting in properly functioning vesicles and maintenance of the synapse. While primary SLCs for the transport of major neurotransmitters like glutamate, GABA, dopamine, serotonin, norepinephrine or acetylcholine are well known and characterized, there are many “orphan” SLCs that are expressed in the brain, the function of which are still poorly understood. One SLC that has recently emerged as a potentially novel monoaminergic and cholinergic vesicular transporter is SLC10A4 (Larhammar et al., 2015).

The human *SLC10A4* gene was first discovered through a bioinformatics approach and a gene expression analysis confirmed expression of SLC10A4 in human brain (Splinter et al., 2006). Robust expression in brain tissue was then validated both in mouse by *in situ* hybridization (Lein et al., 2007) and rat brain by immunohistochemistry (Geyer et al., 2008). Although, Geyer and coworkers (2008) did not elucidate functional properties of SLC10A4, they demonstrated expression of SLC10A4 in cholinergic neurons. They later validated this finding and extended it, reporting co-expression of SLC10A4 with the vesicular monoamine transporter VMAT2 (Burger et al., 2011). At the same time, a gene-expression analysis of dopaminergic neurons in rats confirmed *Slc10a4* mRNA enrichment in midbrain (Zhou et al., 2011).

Although homology analysis has shown that SLC10A4 belongs to the family sodium-bile acid cotransporters, experiments in rat and human cells either failed to confirm transport activity for bile acids or related molecules (Splinter et al., 2006; Geyer et al., 2008), or reported only low bile-acid transport activity for SLC10A4 (Bijsmans et al., 2012; Abe et al., 2013). The first evidence for a function of SLC10A4 in the brain was reported from the Kullander group (Zelano et al., 2013). They showed that mice lacking SLC10A4 had increased sensitivity to cholinergic stimulation resulting in decreased seizure threshold to cholinergic stimuli in hippocampal slices and increased sensitivity to the status epilepticus inducing cholinergic agent pilocarpine. They later went on to demonstrate that SLC10A4 is important for dopamine homeostasis and neuromodulation in vivo, and that mice lacking SLC10A4 are slightly hypoactive and display heightened locomotor sensitivity to the dopamine-releasing drug amphetamine and to tranylcypromine, a monoamine oxidase inhibitor that prevents dopamine degradation (Larhammar et al., 2015).

Here, we extended the scope of *Slc10a4* expression analyses, by quantifying *Slc10a4* mRNA in mouse brain regions identified by previous studies (Lein et al, 2007) and by assessing *Slc10a4* expression in two other major cell types of the brain, astrocytes and microglia. We have also generated a genetic mouse model of SLC10A4 loss by deletion of the *Slc10a4* gene. Using this mouse model, we further examined the consequences of *Slc10a4* loss on cognitive behaviors that are dependent on hippocampal or striatal dopaminergic function

(Darvas and Palmiter, 2010, 2011; Melief et al., 2015), and which have been implicated in neurodegenerative diseases like Parkinson's (Goldman et al., 2013) and Alzheimer's disease (Albert et al., 2011). We further analyzed the effects of deleting *Slc10a4* on brain acetylcholine levels.

EXPERIMENTAL PROCEDURES

Animals

All experiments were approved by the Institutional Animal Care and Use Committee at the University of Washington. The murine *Slc10a4* gene has three exons, all of which contain protein coding regions (Fig. 1A). To generate *Slc10a4* null mice ($Slc10a4^{\Delta/\Delta}$), we first generated $Slc10a4^{lox/lox}$ mice which allow Cre-dependent deletion of the *Slc10a4* gene. $Slc10a4^{lox/lox}$ mice were generated by gene targeting. They have a triple hemagglutinin tag (3xHA) fused to the C-terminus protein coding region of exon 1 and loxP sites flanking exon 2 (Fig. 1B). We crossed $Slc10a4^{lox/lox}$ mice with the B6.129S4-Meox2$^{tm1(cre)Sor}$/J strain (Tallquist and Soriano, 2000) to delete one copy of exon 2 of the *Slc10a4* gene in early embryos ($Slc10a4^{\Delta/+}$, Fig. 1C). Thus generated $Slc10a4^{\Delta/+}$ mice were crossed with C57BL/6J mice to remove the Cre recombinase allele, followed by backcrossing to the C57BL/6J genetic background for 10 generations to generate breeding pairs used for the experiments presented in this manuscript. Only $Slc10a4^{\Delta/+}$ mice were used for breeding and produced litters of wild-type ($Slc10a4^{+/+}$) litter-mate control and $Slc10a4^{\Delta/\Delta}$ mice on a C57BL/6J background. Mice of both genders at the age of 3–5 month were used for all experiments. All mice were housed in groups of 3–5 animals under a 12-h, light-dark cycle (6AM-6PM) in a temperature-controlled environment with food and water available ad libitum.

Reagents

RNA extraction kits (Ambion), TaqMan probes and primers (Applied Biosystems), and penicillin-streptomycin (Gibco) were purchased from Thermo Fisher Scientific (Waltham, MA). The iScript cDNA synthesis kit was purchased from Bio-Rad (Hercules, CA). DMEM/F12 medium and fetal bovine serum were purchased from HyClone (Logan, UT). Papain and DNase I were purchased from Worthington Biochemical (Lakewood, NJ). L-cysteine and poly-L-ornithine were purchased from Sigma-Aldrich (St. Louis, MO).

Slc10a4 expression

Quantification of Slc10a4 mRNA expression in Slc10a4$^{+/+}$ mouse brain—

According to the Allen Mouse Brain Atlas (http://mouse.brain-map.org), *Slc10a4* mRNA is enriched in the striatum, midbrain and brainstem (Lein et al., 2007). To quantify expression of *Slc10a4* mRNA in these brain regions, we collected $Slc10a4^{+/+}$ tissue from striatum, the brain stem, and from the midbrain substantia nigra pars compacta (SNC) and ventral tegmental area (VTA). Tissue was immediately flash-frozen in liquid nitrogen and stored at -70°C. Tissue was homogenized, followed by RNA extraction using Ambion PureLink®RNA kits, and then reverse-transcription with iScript cDNA synthesis kits. TaqMan probes and primers of *Slc10a4* were purchased from Applied Biosystems. Quantitative PCR (qPCR) was performed on an Applied Biosystems ViiA 7 Real-Time PCR

System with the method of relative quantitation (Larionov et al., 2005) using normalization to glyceraldehyde phosphate dehydrogenase (GAPDH) expression (Li et al., 2015) and striatal *Slc10a4* mRNA expression as a calibrator.

Determination of brain cell-types expressing Slc10a4 mRNA—Primary mixed glial cultures were generated from 1- to 3-day-old $Slc10a4^{+/+}$ pups as described previously (Li et al., 2015). In brief, cerebral cortex was dissected from brains and remaining meninges were removed while in ice-cold phosphate-buffered saline (PBS). Cortical tissue was digested by 30-min incubation in DMEM/F12 medium containing papain (15 U/ml), DNase I (200 mg/ml), EDTA (0.5 mM) and L-cysteine (0.2 mg/ml) at 37°C, and then dissociated mechanically. The resulting cell suspension was plated on poly-L-ornithine coated flasks and maintained at 37°C and 5% CO_2 in DMEM/F12 supplemented with 10% fetal bovine serum, penicillin (100 U/ml) and streptomycin (100 μg/ml). After 11–15 days, microglia were collected from the underlying astrocytic monolayer by gentle agitation and replated on poly-L-ornithine-coated plates. After removing microglia, the underlying astrocytes were subcultured in plates coated with poly-L-ornithine. Primary neuron cultures were generated from cerebral cortex of 1-day-old pups as described previously (Li et al., 2013). Cells reaching confluence at 3 days after plating were rinsed twice with ice-cold PBS, collected and flash-frozen in liquid nitrogen. RNA was then isolated, transcribed into cDNA and analyzed for *Slc10a4* expression as described above. *Slc10a4* expression in neuronal cultures was used as calibrator for *Slc10a4* expression in other cell types.

Quantification of Slc10a4 expression in $Slc10a4^{\Delta/\Delta}$ mice—Whole brain RNA from $Slc10a4^{+/+}$ and $Slc10a4^{\Delta/\Delta}$ mice was extracted, transcribed into cDNA and analyzed for *Slc10a4* mRNA expression as described above. *Slc10a4* expression in $Slc10a4^{+/+}$ brain was used as calibrator.

Behavioral studies

All behavior studies were performed in a blinded fashion. The genotypes of all $Slc10a4^{+/+}$ and $Slc10a4^{\Delta/\Delta}$ mice were coded before behavior experiments and maintained coded until completion of all behavioral procedures.

Spatial learning and memory was measured using a modified Barnes maze protocol as previously described (Yang et al., 2013; Melief et al., 2015). Briefly, mice were tested for 4 consecutive days in a Barnes maze apparatus (San Diego Instruments, San Diego, CA) consisting of a 1.0 m disc raised 75 cm off the floor and containing 18 possible escape holes, one of which leads to an escape box. Mice received 4 trials per day with an intertrial interval of 2 mins. Trials lasted until the mouse found the escape box or 5 minutes had elapsed, at which point the mouse was gently shown the escape box. All trials were recorded with a digital video camera. Latency to escape, distance travelled, and errors made (investigations into decoy escape holes) were measured using Any-maze software (Stoelting, Wood Dale, IL). Mice that were tested in the Barnes maze were also tested for locomotor activity, anxiety in the open field and anxiety in the elevated plus maze (see below). These tests were conducted 2 weeks after the Barnes maze procedure.

Locomotor activity in a novel environment was measured using static mouse cages (37.2 cm D × 23.4 cm W × 14 cm H) with 16 photo cells per side (Columbus Instruments) and an IBM computer to record beam breaks. Ambulations (2 consecutive beam breaks) were measured in 5 minute intervals over a 60 minute test period in a novel mouse testing room.

Anxiety and exploration was measured in an open field apparatus and an elevated plus maze. For the open field, a basket 46 cm in diameter was used as the exploration chamber, and animals were allowed to explore for 5 minutes. Time spent in the center zone of the exploration chamber was measured using a digital video camera together with Ethovision software (Leesburg, VA). For the elevated plus maze (St. Albans, VT), time spent in the open arms of the maze was monitored for 10 min using a digital video camera together with Ethovision software (Leesburg, VA).

Egocentric learning, strategy shifting and cue-based learning were measured using in a water U-maze apparatus (Darvas and Palmiter, 2011; Darvas et al., 2014). Mice were released into a gray stem that ended in one black and one white arm choice. One arm always had an escape platform at the end which was not visible to the mice from the stem. The right-left orientation of the arms was alternated in an equal, pseudo-random manner. Mice were given 10 trials per day to learn the location of the escape platform with an intertrial interval of about 5 minutes. Trials lasted until the mouse found the escape platform or 5 minutes had elapsed, at which point the mouse was shown the location of the platform. The first three days of testing, mice were trained to find the escape platform using a directional, turn-based egocentric approach (platform was always to the right or the left, regardless of arm color). Following this training, mice were then challenged with a strategy-shift to a cue-based approach strategy, in which they were trained for five days to find the escape platform using a color based approach (platform was always in the black or the white arm, regardless of direction). Percent correct trials per day and latency to escape were measured. In addition, an independent naïve cohort of mice was trained to learn the cue-based approach strategy over a period of 4 days.

Catecholamine measurements

Animals were sacrificed by rapid decapitation and the brains were removed. 1 mm tissue punches were dissected from the dorsal and ventral striatum (approximately 1.5 mm to -0.5 mm from Bregma). Tissue punches were flash-frozen immediately and stored at -80°C. High-performance liquid chromatography (HPLC) coupled with electrochemical detection (Coulochem III electrochemical detector, Thermo Fisher Scientific, MA) was used to measure dopamine (DA) content and the ratio of 3,4-Dihydroxyphenylacetic acid (DOPAC) to DA content. All raw measurements of DA and DOPAC were normalized to total protein content.

Acetylcholine measurements

Animals were treated with eserine (0.32 mg/kg Sigma-Aldrich, St. Louis, MO) via intraperitoneal injection to preserve acetylcholine (ACh) in tissue. Heads were removed 10 min later, microwaved at full power (1000 W) for 3 seconds to fix tissue, and brains were removed. 1 mm tissue punches were dissected from hippocampus and pedunculopontine

tegmental nucleus (PPTg). Tissue punches were flash-frozen and stored at -80°C. ACh tissue content was determined using a choline/acetylcholine assay kit (Abcam, Cambridge, MA). Fluorescent measures (excitation at 535 nm, emission at 590 nm) were performed using a SpectraMax M2 instrument (Molecular Devices, Sunnyvale, CA) and the ACh content was determined after acetylcholinesterase treatment by subtracting free choline from total choline content. All ACh measurements were normalized to total protein content.

Statistical analysis

All behaviour data analyses used standard repeated-measures (RM) 2-way analysis of variance (ANOVA) together with Sidak's *post-hoc* multiple comparisons test, or Student's t-test when appropriate. Slc10a4 mRNA expression data and ACh data were analysed using one-way ANOVA together with Tukey's *post-hoc* multiple comparisons test, or Student's t-test when appropriate. Striatal DA and DOPAC/DA ratio data were analysed using two-way ANOVA together with Bonferroni's *post-hoc* pair-wise comparison. All data are presented as arithmetic mean and shown together with their respective standard error of mean. Significance was reported when $p < 0.05$.

Results

Slc10a4 expression

We analyzed samples from the striatum (n=8), brain stem (n=10), SNC (n=8) and VTA (n=10) of *Slc10a4*$^{+/+}$ mice (Fig. 2A). ANOVA of *Slc10a4* mRNA expression confirmed significant differences between the analyzed brain regions ($F_{3,32} = 14.6$, $p < 0.01$). Tukey's *post-hoc* test further revealed that *Slc10a4* mRNA expression was significantly higher in brain stem, VTA and SNC when compared with striatum (all $p < 0.05$). Expression in the VTA was also significantly higher than in brain stem and SNC (each $p < 0.05$).

To determine the cell types expressing *Slc10a4*, we cultured primary neurons, astrocytes, and microglia (n=4 for each) from *Slc10a4*$^{+/+}$ mice and measured mRNA levels (Fig. 2B). ANOVA of *Slc10a4* mRNA expression showed significant differences between cell types ($F_{2,9} = 33.12$, $p < 0.01$). Tukey's *post-hoc* test verified that neurons were the primary cell type for *Slc10a4* expression expressing almost 6 fold more mRNA than astrocytes, and almost 30 fold more than microglia (each $p < 0.01$).

Finally, to determine the effectiveness of our *Slc10a4* deletion, we measured *Slc10a4* mRNA in whole brain from *Slc10a4*$^{\Delta/\Delta}$ mice (n = 4) as compared with *Slc10a4*$^{+/+}$ *Slc10a4*$^{+/+}$ mice (n = 6; Fig. 2C). *Slc10a4* mRNA was undetectable in our assays in brains from *Slc10a4*$^{\Delta/\Delta}$ mice, indicating effective deletion of the gene.

Spatial Learning

For all behavioral tasks, we found no differences between male and female mice, and so present the data with genders combined. To assess spatial learning and memory, *Slc10a4*$^{\Delta/\Delta}$ (n = 30) and *Slc10a4*$^{+/+}$ mice (n = 17) were tested in a modified Barnes maze protocol (Fig. 3A). Mice were trained to find the location of an escape box over 4 trials per day for 4 days. Escape latencies to locate the escape box were averaged for each training day. RM 2-way

ANOVA of escape latencies showed significant effects of time ($F_{3, 135} = 9.18$, $p < 0.01$) and genotype ($F_{1, 45} = 7.22$, $p < 0.01$), but not of time-genotype interaction ($F_{3, 135} = 1.85$, $p > 0.05$). Sidak's *post-hoc* multiple comparisons test confirmed a significant impairment by *Slc10a4*$^{\Delta/\Delta}$ mice on the 4th day of testing ($p < 0.01$).

To determine if the observed deficit in spatial learning was due to altered novelty-induced motor activity or anxiety, we further tested subgroups of mice that were previously used in the Barnes maze. Novelty-induced motor activity (Fig. 3B) by *Slc10a4*$^{\Delta/\Delta}$ mice (n = 13) was not different from that of *Slc10a4*$^{+/+}$ mice (n = 12) as indicated by RM 2-way ANOVA of ambulations, which showed significant effects of time ($F_{11, 253} = 66.12$, $p < 0.01$), but not of genotype ($F_{1,23} = 0.17$, $p > 0.05$) or of time-genotype interaction ($F_{11, 253} = 1.02$, $p > 0.05$). There were no significant differences ($p > 0.05$) for time spent in the center of the open field arena (Fig. 3C) between *Slc10a4*$^{\Delta/\Delta}$ (n = 13) and *Slc10a4*$^{+/+}$ mice (n = 8), and also no significant differences ($p > 0.05$) for time spent in the open arm of the elevated plus maze (Fig. 3D) between *Slc10a4*$^{\Delta/\Delta}$ (n = 9) and *Slc10a4*$^{+/+}$ mice (n = 7).

Egocentric learning, strategy shifting and cue-based learning

Given the deficit in spatial learning, we next asked whether *Slc10a4*$^{\Delta/\Delta}$ mice showed deficits in executive function, in particular in cognitive flexibility. A water U-maze apparatus was used to measure a mouse's ability to learn the location of an escape platform using a turn-based escape or a cue-based escape. Both *Slc10a4*$^{+/+}$ (n = 12) and *Slc10a4*$^{\Delta/\Delta}$ mice (n = 16) learned to find the escape platform equally well using the turn-based egocentric learning strategy (Fig. 4A). RM 2-way ANOVA of the percentages of correct trials per training day of the turn-based escape condition confirmed a significant effect of training time ($F_{2, 52} = 48.91$, $p < 0.01$), but not of genotype ($F_{1, 26} = 0.89$, $p > 0.05$) or of time-genotype interaction ($F_{2, 52} = 1.04$, $p > 0.05$).

To assess cognitive flexibility, the same mice were then challenged to find the platform using a cue-based escape after completing the turn-based escape trials (Fig. 4B). RM 2-way ANOVA of the percentages of correct trials per training day of the turn-based escape condition showed a significant effect of training time ($F_{4, 104} = 69.65$, $p < 0.01$), genotype ($F_{1, 26} = 9.7$, $p < 0.01$), but not of time-genotype interaction (c). Sidak's *post-hoc* multiple comparisons test confirmed a significant impairment in *Slc10a4*$^{\Delta/\Delta}$ mice on the 3rd day of testing ($p < 0.01$).

To rule out that the observed deficit in cognitive flexibility was due to impaired cue-based learning, an independent cohort of *Slc10a4*$^{+/+}$ (n = 6) and *Slc10a4*$^{\Delta/\Delta}$ mice (n = 6) trained to find the escape platform using a cue-based learning strategy alone performed equally well as those trained using the turn-based strategy (Fig. 4C). RM 2-way ANOVA of the percentages of correct trials per training day of the turn-based escape condition confirmed only a significant effect of training time ($F_{3, 30} = 41.63$, $p < 0.01$), but not of genotype ($F_{1, 10} = 0.84$, $p > 0.05$) or of time-genotype interaction ($F_{3, 30} = 0.22$, $p > 0.05$).

Tissue Neurotransmitter Content

Because of the enrichment of *Slc10a4* mRNA in the midbrain, we measured the level of DA, the main neurotransmitter of midbrain neurons, and of its metabolite DOPAC in the main

projection field of midbrain neurons, the striatum. Comparison of DA levels in *Slc10a4*$^{+/+}$ (n = 4–5) and *Slc10a4*$^{\Delta/\Delta}$ (n = 8–11) tissue punches from the dorsal and ventral striatum (Fig. 5A) by 2-way ANOVA revealed a significant effect of genotype ($F_{1, 24} = 24.24$, $p < 0.01$), but not of subregion ($F_{1, 24} = 2.04$, $p > 0.05$) or genotype-subregion interaction ($F_{1, 24} = 0.26$, $p > 0.05$). Sidak's *post-hoc* multiple comparisons test confirmed that *Slc10a4*$^{\Delta/\Delta}$ mice had a significantly less DA than *Slc10a4*$^{+/+}$ in both ventral ($p < 0.05$) and dorsal striatum ($p < 0.01$). We then calculated the ratio of DOPAC to DA, which is a measure of dopamine turnover (Fig. 5B). 2-way ANOVA of the DOPAC/DA ratios confirmed significant effects of genotype ($F_{1, 24} = 20.23$, $p < 0.01$), and of subregion ($F_{1, 24} = 4.48$, $p < 0.05$), but not of genotype-subregion interaction ($F_{1, 24} = 0.88$, $p > 0.05$). Sidak's *post-hoc* multiple comparisons test confirmed that *Slc10a4*$^{\Delta/\Delta}$ mice had a significantly increased DOPAC/DA ratio compared with *Slc10a4*$^{+/+}$ in both ventral ($p < 0.01$) and dorsal striatum ($p < 0.05$).

Because of the enrichment of *Slc10a4* mRNA in the brainstem, we measured the levels of acetylcholine, a major neurotransmitter of cholinergic brainstem neurons in the brainstem tissue from *Slc10a4*$^{+/+}$ (n = 8) and *Slc10a4*$^{\Delta/\Delta}$ (n = 7) mice (Fig. 5C). *Slc10a4*$^{\Delta/\Delta}$ mice had significantly reduced ACh levels in the brainstem when compared with *Slc10a4*$^{+/+}$ mice (t-test, $p < 0.01$). Based on previous reports that SLC10A4 protein alters cholinergic function in the hippocampus (Zelano et al., 2013), we also measured acetylcholine levels in the hippocampus of *Slc10a4*$^{+/+}$ (n = 7) and *Slc10a4*$^{\Delta/\Delta}$ (n = 10) mice (Fig. 5D). *Slc10a4*$^{\Delta/\Delta}$ mice had significantly less acetylcholine in the hippocampus than *Slc10a4*$^{+/+}$ mice (t-test, $p < 0.05$).

Discussion

We investigated the effect of genetic deletion of SLC10A4 on motor and cognitive function and neurotransmitter levels in mice. We generated a SLC10A4 knock out mouse using Cre-recombinase targeted deletion of exon 2 to generate *Slc10a4*$^{\Delta/+}$ animals, which were bred to produce *Slc10a4*$^{\Delta/\Delta}$ and *Slc10a4*$^{+/+}$ littermates. Primary cultures of neurons, astrocytes, and microglia were generated from *Slc10a4*$^{+/+}$ neonates to determine expression profiles of *Slc10a4* mRNA, and qPCR of specific regions dissected from adults was used to determine expression profiles in the brain of these animals. We confirmed previous studies identifying midbrain and brainstem regions as being enriched in *Slc10a4* expression (Lein et al., 2007) and determined that neurons were the primary cell type expressing *Slc10a4* in the brain.

We found that homozygous deletion of *Slc10a4* results in reduced DA content in the striatum, and in reduced ACh content in the hippocampus and brainstem, probably related to altered metabolism of these neurotransmitters. Adult animals were then subjected to a battery of behavioral tasks to determine effect of SLC10A4 loss on motor function and cognitive impairment. We found that adult mice displayed impairment in measures of cognitive flexibility and spatial learning, but had no observable motor deficits.

Despite being found to co-localize with the vesicular transporters VMAT2 and VAChT, SLC10A4 has not been found to have any capacity for neurotransmitter transport itself (Schmidt et al., 2015). Our observation of increased dopamine metabolism in the striatum of *Slc10a4*$^{\Delta/\Delta}$ animals is in agreement with previous studies (Larhammar et al., 2015) and

suggests that, rather than act as a solute carrier, as suggested by its homology, SLC10A4 instead somehow regulates neurotransmitter turnover in the synapse. Its association with vesicular transporters supports this hypothesis.

The expression profile of SLC10A4 makes it a target of interest in the study of neurodegenerative diseases. Enrichment in brainstem, loss of ACh in hippocampus and brainstem of *Slc10a4*$^{\Delta/\Delta}$ mice, and localization in cholinergic neurons indicates a potential influence on the misregulation of ACh, one of the primary characteristics of disorders such as Alzheimer's disease (Montine and Montine, 2013). Likewise, enrichment in the midbrain and striatum and its impact on the metabolism of DA indicate a possible role in the pathology of Parkinson's disease. These mice did not demonstrate any overt motor impairment despite a reduction of dopamine in the striatum as compared with wild type animals. We speculate that, with the increase the DOPAC/dopamine ratio seen in these animals, the loss of dopamine reflects a change in dopamine metabolism rather than a "loss" of dopamine, such as would be seen in models of PD. Thus these mice are not a model of PD in and of themselves, but the slight impairment seen in the Barnes maze and the rule-switch portion of the water U-maze task is comparable with the early effects we have seen in a mouse model of Alzheimer's disease with ablated dopamine (Melief et al., 2015). Thus, these animals may provide insights into how misregulation of DA and ACh signaling influences cognitive activity.

The cognitive impairment shown in these mice is limited to a slight delay in learning a rule-switch, which is a measure of cognitive flexibility (Darvas and Palmiter, 2011), while initial learning and memory generally remain intact. This indicates an effect on higher order executive function without impact on more basic cognitive function and might be considered comparable to mild cognitive impairment (MCI) in humans, generally considered a precursor to dementia (Sperling et al., 2011). Of note, these animals were tested at relatively young ages, between 3–5 months. Most animal models of disease do not display cognitive symptoms until later in life, generally over 12 months of age, and thus it may be that what presents as "mild" impairment in these animals may degenerate into more significant impairment with age. Future studies will be needed to determine the effect of SLC10A4 loss on cognitive function in aged animals.

Overall, *Slc10a4*$^{\Delta/\Delta}$ mice display characteristics that mimic early symptoms of neurodegenerative disease. Previous work has suggested that SLC10A4 has a role in synaptic and vesicular function (Geyer et al., 2008; Burger et al., 2011), disruption of which would likely result in impaired neuronal signaling and function. While we do not yet know the status of neuronal health in these animals, the alterations in monoamine and ACh levels coupled with the moderate cognitive impairment suggest that these animals may model brain chemistry imbalance as it contributes to disease. Further studies will be required to explore this possibility.

Acknowledgments

This investigation was supported in part by Howard Hughes Medical Institute (R.D.P.). We thank Ayaka Hulbert for maintaining the mouse colony.

References

Abe T, Kanemitu Y, Nakasone M, Kawahata I, Yamakuni T, Nakajima A, Suzuki N, Nishikawa M, Hishinuma T, Tomioka Y. SLC10A4 is a protease-activated transporter that transports bile acids. J Biochem (Tokyo). 2013; 154:93–101. [PubMed: 23589386]

Albert MS, DeKosky ST, Dickson D, Dubois B, Feldman HH, Fox NC, Gamst A, Holtzman DM, Jagust WJ, Petersen RC, Snyder PJ, Carrillo MC, Thies B, Phelps CH. The diagnosis of mild cognitive impairment due to Alzheimer's disease: recommendations from the National Institute on Aging-Alzheimer's Association workgroups on diagnostic guidelines for Alzheimer's disease. Alzheimers Dement J Alzheimers Assoc. 2011; 7:270–279.

Bijsmans ITGW, Bouwmeester RAM, Geyer J, Faber KN, van de Graaf SFJ. Homo- and hetero-dimeric architecture of the human liver Na^+-dependent taurocholate co-transporting protein. Biochem J. 2012; 441:1007–1015. [PubMed: 22029531]

Burger S, Döring B, Hardt M, Beuerlein K, Gerstberger R, Geyer J. Co-expression studies of the orphan carrier protein Slc10a4 and the vesicular carriers VAChT and VMAT2 in the rat central and peripheral nervous system. Neuroscience. 2011; 193:109–121. [PubMed: 21742018]

Darvas M, Henschen CW, Palmiter RD. Contributions of signaling by dopamine neurons in dorsal striatum to cognitive behaviors corresponding to those observed in Parkinson's disease. Neurobiol Dis. 2014; 65:112–123. [PubMed: 24491966]

Darvas M, Palmiter RD. Restricting dopaminergic signaling to either dorsolateral or medial striatum facilitates cognition. J Neurosci Off J Soc Neurosci. 2010; 30:1158–1165.

Darvas M, Palmiter RD. Contributions of striatal dopamine signaling to the modulation of cognitive flexibility. Biol Psychiatry. 2011; 69:704–707. [PubMed: 21074144]

Geyer J, Fernandes CF, Döring B, Burger S, Godoy JR, Rafalzik S, Hübschle T, Gerstberger R, Petzinger E. Cloning and molecular characterization of the orphan carrier protein Slc10a4: expression in cholinergic neurons of the rat central nervous system. Neuroscience. 2008; 152:990–1005. [PubMed: 18355966]

Goldman JG, Holden S, Bernard B, Ouyang B, Goetz CG, Stebbins GT. Defining optimal cutoff scores for cognitive impairment using Movement Disorder Society Task Force criteria for mild cognitive impairment in Parkinson's disease. Mov Disord Off J Mov Disord Soc. 2013; 28:1972–1979.

Larhammar M, Patra K, Blunder M, Emilsson L, Peuckert C, Arvidsson E, Rönnlund D, Preobraschenski J, Birgner C, Limbach C, Widengren J, Blom H, Jahn R, Wallén-Mackenzie Å, Kullander K. SLC10A4 is a vesicular amine-associated transporter modulating dopamine homeostasis. Biol Psychiatry. 2015; 77:526–536. [PubMed: 25176177]

Larionov A, Krause A, Miller W. A standard curve based method for relative real time PCR data processing. BMC Bioinformatics. 2005; 6:62. [PubMed: 15780134]

Lein ES, et al. Genome-wide atlas of gene expression in the adult mouse brain. Nature. 2007; 445:168–176. [PubMed: 17151600]

Lin L, Yee SW, Kim RB, Giacomini KM. SLC transporters as therapeutic targets: emerging opportunities. Nat Rev Drug Discov. 2015; 14:543–560. [PubMed: 26111766]

Li X, Montine KS, Keene CD, Montine TJ. Different mechanisms of apolipoprotein E isoform–dependent modulation of prostaglandin E2 production and triggering receptor expressed on myeloid cells 2 (TREM2) expression after innate immune activation of microglia. FASEB J. 2015; 29:1754–1762. [PubMed: 25593125]

Li X, Rose S, Montine K, Keene CD, Montine TJ. Antagonism of Neuronal Prostaglandin E2 Receptor Subtype 1 Mitigates Amyloid β Neurotoxicity In Vitro. J Neuroimmune Pharmacol Off J Soc NeuroImmune Pharmacol. 2013; 8:87–93.

Melief EJ, Cudaback E, Jorstad NL, Sherfield E, Postupna N, Wilson A, Darvas M, Montine KS, Keene CD, Montine TJ. Partial depletion of striatal dopamine enhances penetrance of cognitive deficits in a transgenic mouse model of Alzheimer's disease. J Neurosci Res. 2015; 93:1413–1422. [PubMed: 25824456]

Montine KS, Montine TJ. Anatomic and Clinical Pathology of Cognitive Impairment and Dementia. J Alzheimers Dis. 2013; 33:S181–S184. [PubMed: 22699849]

Schmidt S, Moncada M, Burger S, Geyer J. Expression, sorting and transport studies for the orphan carrier SLC10A4 in neuronal and non-neuronal cell lines and in Xenopus laevis oocytes. BMC Neurosci. 2015; 16:35. [PubMed: 26084360]

Sperling RA, et al. Toward defining the preclinical stages of Alzheimer's disease: Recommendations from the National Institute on Aging-Alzheimer's Association workgroups on diagnostic guidelines for Alzheimer's disease. Alzheimers Dement. 2011; 7:280–292. [PubMed: 21514248]

Splinter P-L, Lazaridis K-N, Dawson P-A, LaRusso N-F. Cloning and expression of SLC10A4, a putative organic anion transport protein. World J Gastroenterol. 2006; 12:6797–6805. [PubMed: 17106928]

Tallquist MD, Soriano P. Epiblast-restricted Cre expression in MORE mice: a tool to distinguish embryonic vs. extra-embryonic gene function. Genes N Y N 2000. 2000; 26:113–115.

Yang Y, Cudaback E, Jorstad NL, Hemingway JF, Hagan CE, Melief EJ, Li X, Yoo T, Khademi SB, Montine KS, Montine TJ, Keene CD. APOE3, but Not APOE4, Bone Marrow Transplantation Mitigates Behavioral and Pathological Changes in a Mouse Model of Alzheimer Disease. Am J Pathol. 2013; 183:905–917. [PubMed: 23831297]

Zelano J, Mikulovic S, Patra K, Kühnemund M, Larhammar M, Emilsson L, Leao R, Kullander K. The synaptic protein encoded by the gene Slc10A4 suppresses epileptiform activity and regulates sensitivity to cholinergic chemoconvulsants. Exp Neurol. 2013; 239:73–81. [PubMed: 23022458]

Zhou Q, Li J, Wang H, Yin Y, Zhou J. Identification of nigral dopaminergic neuron-enriched genes in adult rats. Neurobiol Aging. 2011; 32:313–326. [PubMed: 19303663]

- *Slc10a4* expression is enriched in midbrain and brainstem regions
- *Slc10a4*$^{\Delta/\Delta}$ mice have moderate impairment in spatial learning and cognitive flexibility
- Dopamine and acetylcholine levels are reduced in *Slc10a4*$^{\Delta/\Delta}$ mice

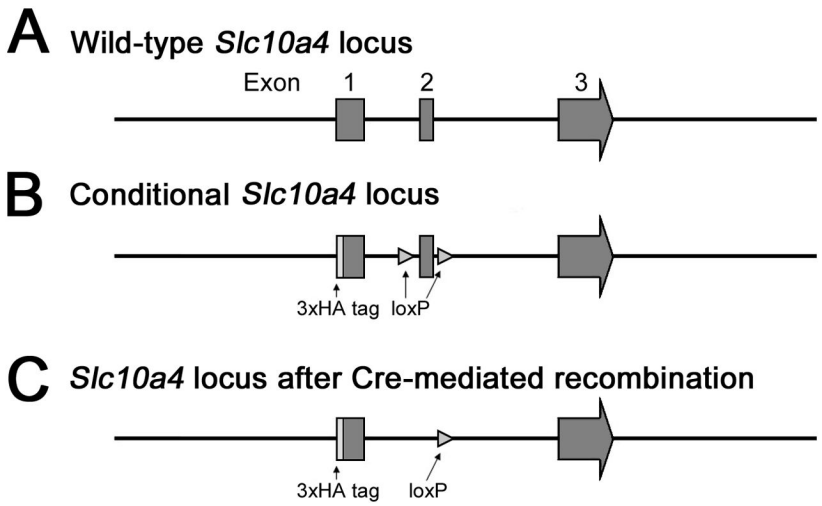

Figure 1.

Targeting strategy for generation of *Slc10a4*$^{\Delta/\Delta}$ and *Slc10a4*$^{\Delta/+}$ mice. A) Wild type *Slc10a4* locus. B) Conditional *Slc10a4* with loxP sites flanking Exon 2. C) *Slc10a4*$^{\Delta}$ locus lacking Exon 2 after Cre excision.

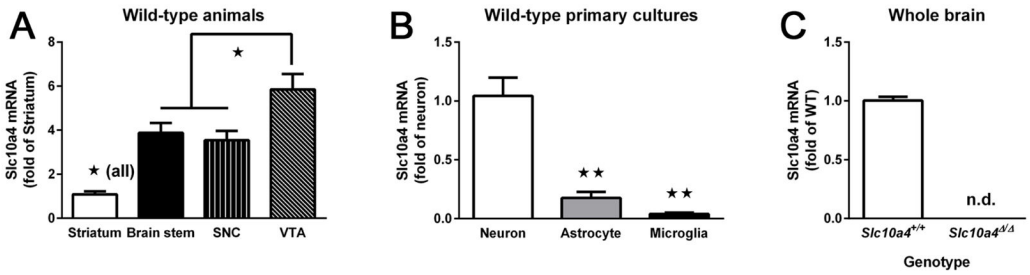

Figure 2.

Expression of *Slc10a4* mRNA. A) In *Slc10a4*$^{+/+}$ brain regions *Slc10a4* mRNA was enriched in brainstem, substantia nigra (SNc), and ventral tegmental area (VTA) (ANOVA with Tukey's post hoc comparison, *p<0.05). B) In primary culture cell types, *Slc10a4* mRNA was preferentially expressed in neurons, with significantly less expression in astrocytes and microglia (ANOVA with Tukey's post hoc comparison, **p<0.01). C). Whole brain analysis of *Slc10a4* mRNA shows the lack of expression in *Slc10a4*$^{\Delta/\Delta}$ mice as compared with *Slc10a4*$^{+/+}$ littermates.

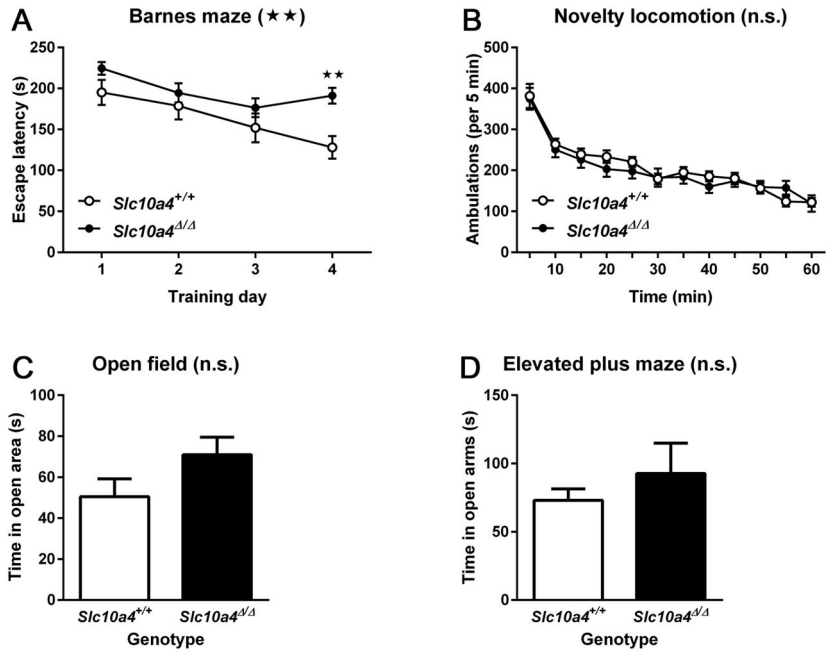

Figure 3.

Learning, novelty induced and anxiety-related behaviors. A) *Slc10a4*$^{\Delta/\Delta}$ mice had a significantly increased latency to find the escape box on the 4th day of a Barnes maze protocol as compared with *Slc10a4*$^{+/+}$ animals (ANOVA with Sidak's post hoc comparison test, *p<0.05). Despite this, there was no difference between these genotypes in B) novelty-induced locomotor activity, C) open field exploration, and D) open arm exploration of an elevated plus maze.

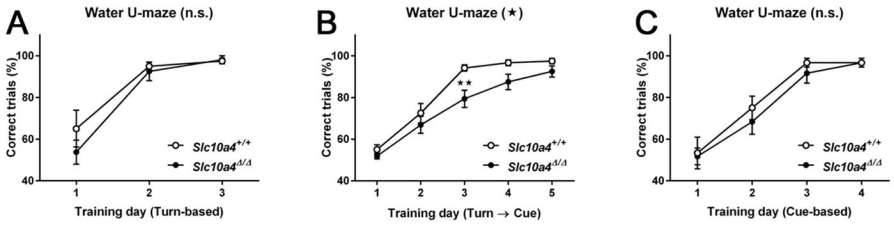

Figure 4.

Strategy-shift water U-maze. A) *Slc10a4*$^{\Delta/\Delta}$ and *Slc10a4*$^{+/+}$ mice did not differ in number of correct trials to learn the turn-based location of an escape platform. B) *Slc10a4*$^{\Delta/\Delta}$ mice were significantly impaired at learning a new cue-based location of the escape platform after turn-based training as compared with *Slc10a4*$^{+/+}$ littermates (2-way ANOVA with Sidak's post hoc comparison test, **p<0.01). C) As a control, *Slc10a4*$^{\Delta/\Delta}$ and *Slc10a4*$^{+/+}$ mice were equally able to learn the location of the escape platform using a cue-based strategy by itself.

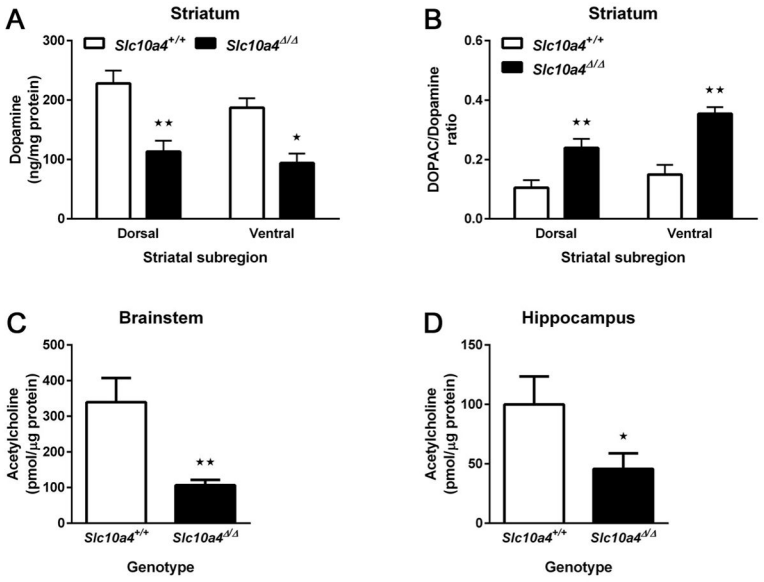

Figure 5.

Dopamine and acetylcholine content. A) *Slc10a4*$^{\Delta/\Delta}$ mice had significantly reduced dopamine content measured by HPLC analysis in both the dorsal and ventral striatum as compared with *Slc10a4*$^{+/+}$ mice (2-way ANOVA with Sidak's post hoc comparison test, *p<0.05, **p<0.01). B) By comparison, *Slc10a4*$^{\Delta/\Delta}$ mice had increased DOPAC concentrations in the same regions (2-way ANOVA with Sidak's post hoc comparison test, *p<0.05, **p<0.01). Additionally, ACh was reduced in *Slc10a4*$^{\Delta/\Delta}$ mice in both B) the brainstem (t-test, **p<0.01) and C) the hippocampus as compared with *Slc10a4*$^{+/+}$ mice (t-test, *p<0.05).